Materials Research Letters

ISSN: (Print) 2166-3831 (Online) Journal homepage: https://www.tandfonline.com/loi/tmrl20

Operando diagnostic detection of interfacial oxygen 'breathing' of resistive random access memory by bulk-sensitive hard X-ray photoelectron spectroscopy

Gang Niu, Pauline Calka, Peng Huang, Sankaramangalam Ulhas Sharath, Stefan Petzold, Andrei Gloskovskii, Karol Fröhlich, Yudi Zhao, Jinfeng Kang, Markus Andreas Schubert, Florian Bärwolf, Wei Ren, Zuo-Guang Ye, Eduardo Perez, Christian Wenger, Lambert Alff & Thomas Schroeder

To cite this article: Gang Niu, Pauline Calka, Peng Huang, Sankaramangalam Ulhas Sharath, Stefan Petzold, Andrei Gloskovskii, Karol Fröhlich, Yudi Zhao, Jinfeng Kang, Markus Andreas Schubert, Florian Bärwolf, Wei Ren, Zuo-Guang Ye, Eduardo Perez, Christian Wenger, Lambert Alff & Thomas Schroeder (2019) *Operando* diagnostic detection of interfacial oxygen 'breathing' of resistive random access memory by bulk-sensitive hard X-ray photoelectron spectroscopy, Materials Research Letters, 7:3, 117-123, DOI: 10.1080/21663831.2018.1561535

To link to this article: https://doi.org/10.1080/21663831.2018.1561535

MATER. RES. LETT.
2019, VOL. 7, NO. 3, 117–123
https://doi.org/10.1080/21663831.2018.1561535

MATERIALS RESEARCH LETTERS
Taylor & Francis
Taylor & Francis Group

ORIGINAL REPORT

Operando diagnostic detection of interfacial oxygen 'breathing' of resistive random access memory by bulk-sensitive hard X-ray photoelectron spectroscopy

Gang Niu[a], Pauline Calka[b], Peng Huang[c], Sankaramangalam Ulhas Sharath[d], Stefan Petzold[d], Andrei Gloskovskii[e], Karol Fröhlich[f], Yudi Zhao[c], Jinfeng Kang[c], Markus Andreas Schubert[b], Florian Bärwolf[b], Wei Ren[a], Zuo-Guang Ye[g,a], Eduardo Perez[b], Christian Wenger[b], Lambert Alff[c] and Thomas Schroeder[b,h]

[a]Electronic Materials Research Laboratory, Key Laboratory of the Ministry of Education & International Center for Dielectric Research, School of Electronic and Information Engineering, Xi'an Jiaotong University, Xi'an, People's Republic of China; [b]IHP, Im Technologiepark 25, Frankfurt, Germany; [c]Institute of Microelectronics, Peking University, Beijing, People's Republic of China; [d]Institute of Materials Science, Technische Universität Darmstadt Darmstadt, Germany; [e]Deutsches Elektronen-Synchrotron DESY Hamburg, Germany; [f]Institute of Electrical Engineering, Slovak Academy of Sciences Bratislava, Slovakia; [g]Department of Chemistry and 4D LABS, Simon Fraser University, Burnaby, Canada; [h]Brandenburgische Technische Universität, Cottbus, Germany

ABSTRACT

The HfO_2-based resistive random access memory (RRAM) is one of the most promising candidates for non-volatile memory applications. The detection and examination of the dynamic behavior of oxygen ions/vacancies are crucial to deeply understand the microscopic physical nature of the resistive switching (RS) behavior. By using synchrotron radiation based, non-destructive and bulk-sensitive hard X-ray photoelectron spectroscopy (HAXPES), we demonstrate an operando diagnostic detection of the oxygen 'breathing' behavior at the oxide/metal interface, namely, oxygen migration between HfO_2 and TiN during different RS periods. The results highlight the significance of oxide/metal interfaces in RRAM, even in filament-type devices.

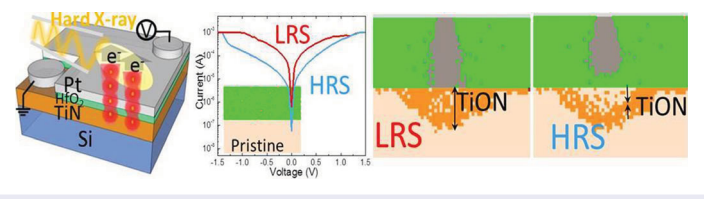

IMPACT STATEMENT

The oxygen 'breathing' behavior at the oxide/metal interface of filament-type resistive random access memory devices is operandoly detected using hard X-ray photoelectron spectroscopy as a diagnostic tool.

ARTICLE HISTORY
Received 15 September 2018

KEYWORDS
HAXPES; resistive switching; interface; RRAM; HfO_2

1. Introduction

Resistive switching (RS) behavior in a simple metal-insulator-metal (MIM) structure has attracted intensive interests, initially for the non-volatile memory and logic applications [1] and has recently been extended to memristive devices and neuromorphic computing applications, e.g. synapse emulators [2], to realize logic-in-memory concepts [3]. Among the resistive random access memory (RRAM) candidates, valence change memories (VCMs) show a great potential thanks to their virtues such as non-volatile (10^6 s), fast (< 10 ns) and low-power (1 pJ/bit) operation [4]. Particularly, the HfO_2-based RRAMs possess the compatibility with the current semiconductor fabrication process, which makes the large scale, low-cost integrated chips fabrication possible [5]. It is widely accepted that filament-type VCMs showing resistive switching (RS)-independence of cell area are superior for the device scaling [6]. However, even for the filament-type devices, in-situ TEM observation and many other studies clearly demonstrate that the

CONTACT Gang Niu gangniu@xjtu.edu.cn Electronic Materials Research Laboratory, Key Laboratory of the Ministry of Education & International Center for Dielectric Research, School of Electronic and Information Engineering, Xi'an Jiaotong University, Xi'an 710049, People's Republic of China; Thomas Schroeder thomas.schroeder@ikz-berlin.de Brandenburgische Technische Universität, Konrad-Zuse-Strasse 1, 03046 Cottbus, Germany

Supplemental data for this article can be accessed here. https://doi.org/10.1080/21663831.2018.1561535

metal–insulator interfaces play also a key role in impacting the RS behavior [7–10]. For instance, metal electrodes such as Ti or TiN serve as oxygen reservoirs, which strongly influence the $V_o^{\bullet\bullet}$ formation and recombination such that suitable interface tailoring could possibly modify RS behavior ranging from a clockwise (CW) bipolar RS (BRS) to a counter-clockwise (CCW) BRS one, or to even a complementary RS (CRS) [8,11]. Moreover, for those memristive applications like synapse simulation, it was suggested that the electrode oxidation/de-oxidation at the interface is important [9]. In order to better optimize and design HfO_2-based RRAM-related devices, it is of great significance to examine the metal–oxide interface in a diagnostic way during the RS process and thoroughly understand the material modification at the interface, particularly the dynamic behavior of the oxygen ions.

X-ray photoelectron spectroscopy (XPS) has been proven as a powerful non-destructive tool to study the physico-chemical properties of material surfaces. Nonetheless, conventional XPS ($h\nu < 2$ keV) is limited to the probing depth of 1–2 nm. Synchrotron radiation based hard X-ray photoelectron spectroscopy (HAXPES) using high excitation energies thus having larger inelastic mean free path (IMFP) of the excited electrons and larger probing depth [12], allows bulk sensitive physico-chemical analysis of the interface details of MIM or metal–oxide-semiconductor (MOS) structures. Our group have reported *operando* HAXPES studies on the top interface of Ti/HfO_2/TiN heterostructure and clarified the gettering role of the Ti top electrode [13–15]. However, although it is widely accepted that the TiN could also play a role of oxygen reservoir and TiN oxidation could strongly modify the RS behavior of RRAM devices [8,16], the impact of the bottom TiN electrode is still not fully clear. Changing the Ti top electrode to Pt which does not contain Ti as in TiN would permit the possible detection of HfO_2/TiN interface. Moreover, the Pt/HfO_2/TiN heterostructure has been considered as a prototype RRAM system [8–11,16] thanks to its good RS properties.

In this work, we present an *operando* investigation of the material property modification of the Pt/HfO_2/TiN MIM system at each resistance state during the RS process. The bulk sensitive feature of the HAXPES permits detection passing through all the way down to the bottom electrode of TiN and therefore allows the clarification of the migration of oxygen atoms in the whole MIM heterostructure during RS.

2. Experiments

The TiN layers were deposited Si (001) as the bottom electrode. Subsequently, 5 nm-thick HfO_2 thin films were grown by atomic layer deposition (ALD), using the $Hf[N(CH_3)(C_2H_5)]_4$ precursor at 300°C and ozone (O_3). Then 9 nm-thick Pt films were deposited as the top electrode. The crystallinity of the films was examined by transmission electron microscopy (TEM) using a FEI Tecnai Osiris equipment. For HAXPES experiments, the Pt/HfO_2/TiN/Si (001) samples were firstly cut into small pieces with an area of $700 \times 700\ \mu m^2$. HAXPES measurements were performed at the P09 beamline of PETRA III at DESY. The excitation energy of the photon source was 8 keV. The X-ray spot size was $\sim 200\ \mu m$ in diameter. The base pressure in the HAXPES chamber was 10^{-9} mbar. More experimental details can be found in Supplemental Information.

3. Results and discussion

Figure 1 shows the Pt/HfO_2/TiN heterostructure characterized by TEM and electron dispersive X-ray spectroscopy (EDX). Figure 1(a) exhibits a cross-sectional view of the TEM image for the heterostructure. The HfO_2 film is flat, smooth and mainly amorphous. Pt forms a complete and flat layer (Supplemental Information). This helps avoid any local roughness effect. Figure 1(b) shows a compositional line profile of atomic concentrations obtained by EDX scanning along the white line marked in Figure 1 (a). It can be seen that below spot 2, the oxygen signal decreases much faster than the Hf signal, suggesting a rather oxygen deficient 2–3 nm–thick HfO_x layer. Further down toward spot 3, both Ti and N signals strongly augment and the O signal decreases slowly, indicating the partial oxidation of TiN surface and an inter-diffusion of HfO_x and TiON. It is noted here that, nitrogen impurities in the HfO_2 layer could possibly impact the reliability (e.g. endurance) and the working current of RRAM devices due to the possible interaction of nitrogen atoms and oxygen vacancies in HfO_2 [17]. However, the oxygen migration is till dominating during RS [7,11,18]. It should also be pointed out that the TiN surface was already partly oxidized prior to the growth of HfO_2 (Supplemental Information).

A RRAM device with the structure shown in Figure 1(c) was fabricated and characterized by HAXPES. HAXPES could largely increase the detection depth down to the TiN bottom electrode, based on the theoretical estimation using the TPP-2 equation [19]. Figure 1(d) indicates the typical current–voltage (I–V) characteristics of the device operating at PETRA III. The inset demonstrates the forming process of the device with a forming voltage (V_F) of −5.4 V. After forming, the device could be switched properly with a compliance current I_{cc} of 10^{-3} A, as shown in Figure 1(d), where the high

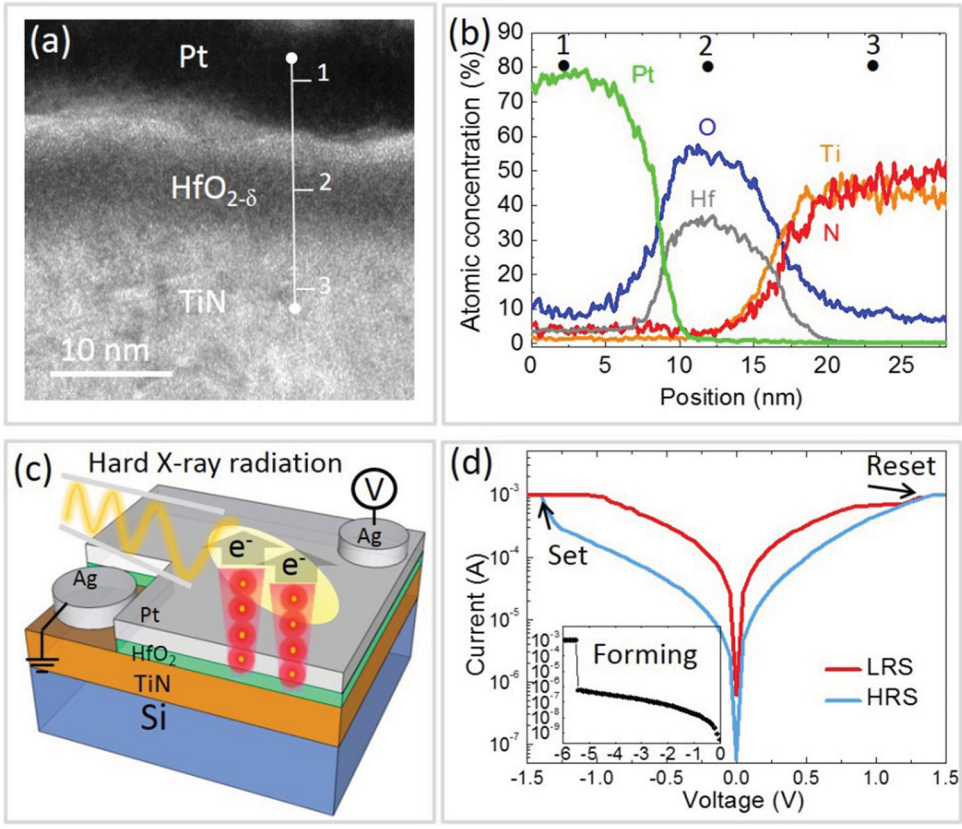

Figure 1. (a) A cross-sectional TEM image on the Pt/HfO_2/TiN heterostructure. (b) A compositional line profile by EDX obtained along the white line in (a). (c) Schematic illustration of the RRAM device structure and HAXPES detection. (d) *I–V* characteristics of the device shown in (a); the inset shows the forming process.

resistance state (HRS) and low resistance state (LRS) processes were marked by blue and red curves, respectively. The 'Set' voltage (V_{set}) and 'Reset' voltage (V_{Reset}) are ~ -1.3 V and ~ 1.2 V, respectively. Compared to the generally reported RS values of HfO_2-related devices with a device area of $< 100 \times 100\ \mu m^2$ [20], the V_{Set} and V_{Reset} values are quite similar, indicating that the HfO_2 RRAM devices are filament-type and the RS voltages being related to local CFs are device area independent [6,20].

Operando HAXPES measurements were then carried out and the results were shown in Figure 2(a–c), where four RS states, i.e. Pristine, Formed, HRS and LRS were shown from the bottom to the top. It should be noted here that in the survey spectrum (Supplemental Information), the Pt peaks originated from the top Pt electrode are the strongest. And the Ti and N XPS peaks of the bottom TiN also appear thanks to the high detection depth of the hard X-ray of 8 keV. Both the Pt 4f and the valence band peaks of the virgin state show no change after the electroforming and at different RS states (Supplemental Information), which indicates that Pt remains inert with no oxidation during the whole RS process. Due to the impact of strong Pt spectra, all the spectra were analyzed by subtracting a linear background.

Figure 2(a) exhibits the Hf 4f spectra, which were fitted by two series of doublets, i.e. HfO_2 (Hf^{4+}, dark green) and HfO_x ($x = 1$ or 3/2, corresponding to Hf^{2+} or Hf^{3+}, light green). In both series, the distance between Hf 4f 5/2 (at higher binding energy, BE) and Hf 4f 7/2 (at lower BE) components was set to 1.68 eV [21] and the area ratio of them was set to 3:4. It can be evidently observed that the HfO_x components appear to be dominant for the four RS states, even at the Pristine state, which indicates that the HfO_2 film is partly oxygen deficient after the growth. This result is in line with the observation by TEM-EDX (Figure 1). Comparing the Formed Hf 4f spectrum with the Pristine one, it can be seen that the spectrum profile changes, particularly at BE $\sim$ 19 eV and the relative height of the peak at BE $\sim$ 18.2 eV decreases (marked by arrows in Formed Hf 4f spectrum). Slight variation can also be observed for the HRS and LRS states. In order to further understand such variation, the area concentration of the components was calculated and shown quantitatively in Figure 2(d), in which the broken line marks the HfO_2 concentration of Pristine state, $\sim$30%. Obviously,

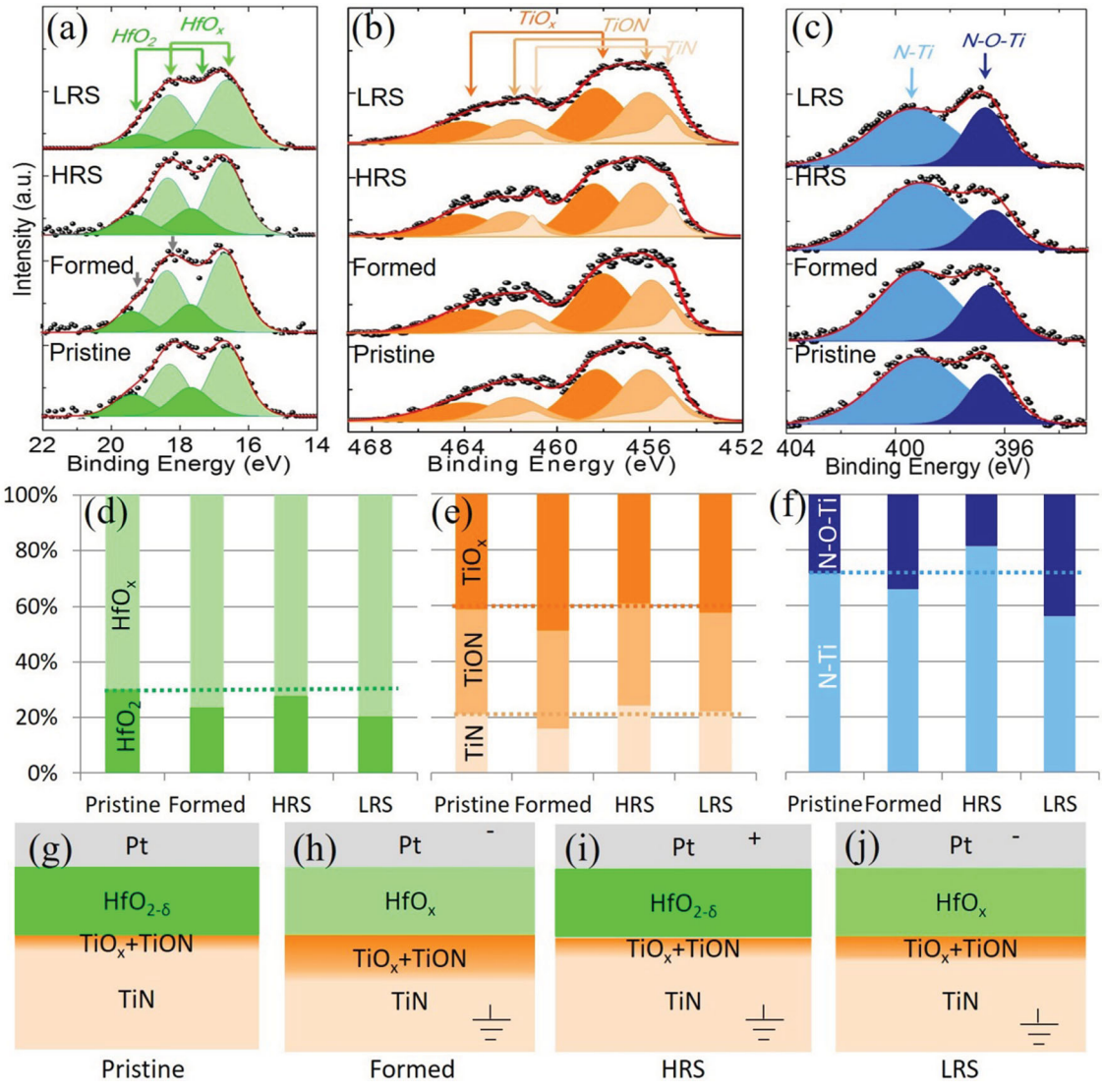

Figure 2. HAXPES results of (a) Hf 4f; (b) Ti 2p; (c) N1s. Figures from the bottom to the top correspond to the RS states of Pristine, Formed, HRS and LRS, respectively. Black dots are experimental data, the red line indicates the fitting profile and the peaks with different colors are fitted peaks for ions with different valence states. (d–f) show the comparison of the component area concentrations for Hf, Ti and N, respectively. (g–j) schematically demonstrate the variation of oxides at the Pristine, Formed, HRS and LRS states, respectively. CFs were not drawn here.

the HfO_2 concentration decreases to ~22% after forming, then it increases to ~29% at HRS after Reset, and then decreases again to ~20% at LRS after 'Set'.

Figure 2(b) exhibits the analyzed Ti 2p HAXPES data, fitted by three series of doublets, i.e. TiO_x (dark orange), TiON (middle orange) and TiN (light orange), respectively. Similarly to all other peaks, the TiO_x and TiON components were fitted by Gaussian–Lorentzian (G–L) functions, with spin–orbit splitting of 5.7 eV. Nevertheless, the TiN components were fitted by Doniach–Sunjic (D–S) functions with a pair of 'tails' at higher BE of the corresponding D–S lines [22] and the spin–orbit splitting is 6.0 eV. The D-S functions were commonly used for the XPS peaks obtained from metals while the satellites at higher BE are related to unscreened final states of TiN [22]. Figure 2(e) displays more details about the variation of the concentrations of the three components. The light orange and dark orange broken lines mark the levels of the TiN and TiO_x components at the Pristine state, respectively. When the state changes from Pristine to Formed, to HRS and then to LRS, the TiN concentration decreases from 20% to 17%, then increases to 21% and decreases again to 20%, whereas the TiO_x concentration firstly increases from 40% to 48%, then decreases to 40% and finally increases back to 43%. These results evidently suggest that the electroforming process drives the oxygen ions from the HfO_2 layer to the TiN bottom electrode. Thus, the TiN surface was oxidized to TiON and TiO_x

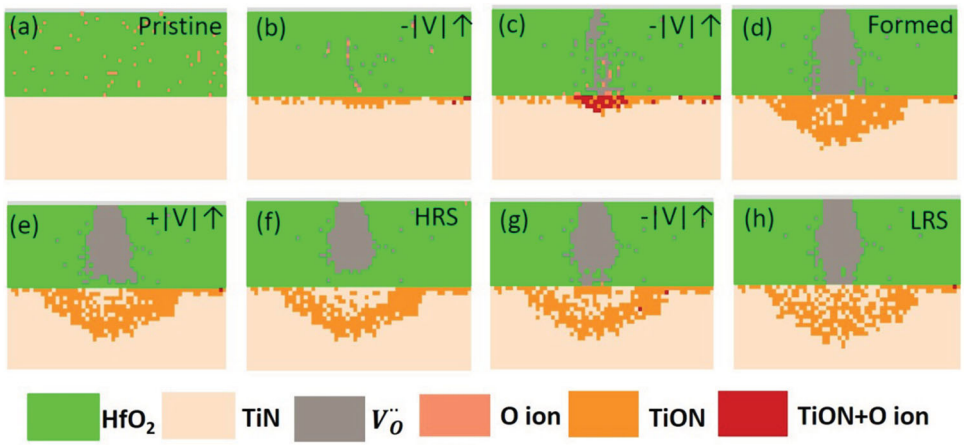

Figure 3. Monte Carlo simulations of the simplified system to show the shift of oxygen ions: (a) Pristine state; (b) a negative bias applied; (c) the negative bias further increased; (d) Formed state; (e) a positive bias applied; (f) HRS state; (g) a negative bias applied and (h) LRS state.

from the Pristine to the Formed state. It is known that the oxidation of TiN electrode leads firstly to TiON and then to TiO_x under even richer oxygen environment [23]. The 'Reset' process promotes the oxygen ions migration from the oxidized TiN back to HfO_2 layer (HRS state) while the Set process drives the oxygen ions again from the HfO_2 layer back to the TiN oxygen reservoir.

This scenario can be further confirmed by analyzing N 1s spectra. Figure 2(c) shows the N 1s spectra fitted by the N-Ti (light blue) and N-O (dark blue) components and the concentration variation of both components as a function of RS states was shown in Figure 2(f). The blue broken line marks the level of N-O at the Pristine state and apparently N-O increases after forming, decreases at HRS and then increases again at LRS. It is noted that O 1s spectra were also collected, which are however, strongly impacted by organic C–O related bonds thus cannot be used for analysis (Supplemental Information). It has to be noted here that the observed changes do not drive the resistance change because the Pt/HfO_2/TiN RRAM device is filament-type [7,10] and the conductive filament dominates the resistance changes during the switching.

The different states of the Pt/HfO_2/TiN heterostructure was schematically illustrated in Figure 2(g–j) for different RS states. At the Pristine state (g), the surface of the TiN bottom electrode was partially oxidized to TiO_x and TiON and there were some oxygen vacancies $V_o^{\bullet\bullet}$ existing in the $HfO_{2-\delta}$ film. At the Formed state (h), numerous $V_o^{\bullet\bullet}$ were created due to the migration of oxygen ions to the TiN electrode, where a thicker oxidized (TiON + TiO_x) layer was formed. At the HRS state after 'Reset' (i), the oxygen ions with negative charges were absorbed back into the HfO_x layer to form the $HfO_{2-\delta}$ layer. At the LRS state after 'Set' (j), the negatively charged oxygen ions were pushed back again into the TiN reservoir layer and $V_o^{\bullet\bullet}$ was formed in the HfO_x layer. It is noted that the CFs dominating the RS process, were not described in the model because HAXPES does only globally detect interface chemistry phenomena and spatially resolved spectro-microscopy HAXPES studies for HfO_2-based RRAM are still beyond the state-of-the-art, despite a recent report visualizing the switching filament in a $SrTiO_3$-based RRAM system using hard X-ray [24].

In order to clarify the oxygen 'breathing' behavior at the HfO_2/TiN interface by considering the RS mechanism in the context of the CF mechanism of the HfO_2-based RRAM, the RS process was analyzed by Monte Carlo simulations based on a physical model[7,25] (more details in Supplemental Information). Since HAXPES cannot examine the local materials modification in the nm-sized CFs, but rather globally the whole area under the X-ray spot with a diameter of $\sim$200 µm, our simulation was mainly focused on the materials modification at the interfaces. The simulated device structure was set to be exactly the same as the examined device with a Pt/HfO_2/TiN structure, as shown in Figure 3(a). With the increase of the negative bias during the forming process, $V_o^{\bullet\bullet}$ as generated and the oxygen ions shifted into TiN and stored in the form of TiON. It is worth noting here that evidently the whole surface of the TiN layer was oxidized to TiON and the TiON thickness increased with the augmentation of the applied bias, which is in line with the HAXPES observation. (TiO_x was not considered here for simplification.) Then, gradually a CF started forming to connect both electrodes (Figure 3(b)). The CF broadened and more and more TiON was formed due to the migration of the oxygen anions into the TiN layer, with the further increase of forming voltage (Figure 3(c)) till the 'Formed' state (Figure 3(d)). In Figure 3(e), a positive

bias was applied and the Reset was carried out, the TiON in the TiN layer commenced releasing oxygen ions into the HfO_x layer and the rupture of CF began. At the HRS state (Figure 3(f)), the CF was broken and oxygen ions majorly moved back into the HfO_2 layer. With the ongoing of 'Set' process under the negative bias, the CF was built up again and the amount of oxygen ions in the TiN largely augmented till the device reached the LRS state (Figure 3(h)). Here, both CF shape and its rupture location were not considered. The simulations based on the physical model describe only the movement of oxygen ions, which confirms well the HAXPES results.

4. Conclusion

In conclusion, synchrotron radiation based, bulk sensitive HAXPES method was used to *operando* evaluate the Pt/HfO_2/TiN RRAM device and it has been shown to be a strong diagnostic tool to clarify the physico-chemical properties of the materials in the device at different operating RS states. Although the RS of HfO_2 RRAM devices are dominated by the formation and rupture of CFs, it is revealed that the RS process is accompanied with the 'breathing' behavior of oxygen at the HfO_2/TiN interface. Compared to the Pt electrode, the TiN electrode plays a more dominating role in RS by 'inhaling' oxygen during the Forming and Set states, and 'exhaling' oxygen during 'Reset' process. The HAXPES diagnostic method demonstrated in this work enriches the microscopic physical understanding of the RS mechanism of the RRAM devices, which certainly facilitates the possible regulation of RS modes and thus the further optimization of device performances.

Acknowledgements

The authors gratefully thank the technical assistance from Dr. Jan Soltys and Dr. Winfried Seifert during the device preparation.

Disclosure statement

No potential conflict of interest was reported by the authors.

Funding

We acknowledge the funding support from Deutsche Forschungsgemeinschaft (DFG, RRAM project SCHR 1123/7-2 and AL 560/13-2), Natural Science Foundation of China (grant number 51602247), Natural Science Fundamental Research Project of Shaanxi Province of China (No. 2017JQ6003), the Fundamental Research Funds for the Central Universities and the Natural Sciences and Engineering Research Council of Canada (NSERC DG grant number 203773).

ORCID

Zuo-Guang Ye http://orcid.org/0000-0003-2378-7304

References

[1] Waser R, Aono M. Nanoionics-based resistive switching memories. Nat Mater 2007;6:833–840
[2] Berdan R, Vasilaki E, Khiat A, et al. Emulating Short-Term Synaptic Dynamics with memristive devices. Sci Rep. 2016;6:18639
[3] Huang P, Kang J, Zhao Y, et al. Reconfigurable Nonvolatile logic Operations in resistance switching Crossbar Array for large-scale Circuits. Adv Mater. 2016;28(44):9758–9764
[4] Waser R. Nanoelectronics and Information Technology. Berlin: Wiley-VCH; 2012.
[5] Mistry K, Allen C, Auth C, et al. A 45 nm Logic Technology with High-k + Metal Gate Transistors, Strained Silicon, 9 Cu Interconnect Layers, 193 nm Dry Patterning, and 100% Pb-free Packaging. 2007 IEEE International Electron Devices Meeting (IEDM). 2007;247-250
[6] Sawa A. Resistive switching in Transition metal oxides. Mater Today. 2008;11(6):28–36
[7] Li C, Gao B, Yao Y, et al. Direct observations of nanofilament evolution in switching processes in HfO_2-based resistive random access memory by in situ TEM studies. Adv Mater. 2017. 1602976-n/a
[8] Brivio S, Frascaroli J, Spiga S. Role of metal-oxide interfaces in the Multiple resistance switching Regimes of Pt/HfO_2/TiN devices. Appl Phys Lett. 2015;107(2):023504
[9] Brivio S, Covi E, Serb A, et al. Experimental study of Gradual/abrupt Dynamics of HfO_2-based memristive devices. Appl Phys Lett. 2016;109(13):133504
[10] Boris H, Wang IT, Wei-Li L, et al. Interface Engineered HfO_2 -based 3D Vertical ReRAM. J Phys D Appl Phys. 2016;49(21):215102
[11] Sharath SU, Vogel S, Molina-Luna L, et al. Control of switching modes and Conductance Quantization in oxygen Engineered HfOx based memristive devices. Adv Funct Mater. 2017;27(32):1700432.
[12] Jablonski A, Powell CJ. Relationships between electron inelastic mean free paths, effective attenuation lengths, and mean escape depths. J Electron Spectrosc Relat Phenom. 1999;100(1):137–160
[13] Bertaud T, Sowinska M, Walczyk D, et al. In-Operando and Non-destructive analysis of the resistive switching in the Ti/HfO_2/TiN-based system by hard X-Ray photoelectron spectroscopy. Appl Phys Lett. 2012;101:143501
[14] Sowinska M, Bertaud T, Walczyk D, et al. In-operando hard X-ray photoelectron spectroscopy study on the impact of current compliance and switching Cycles on oxygen and Carbon Defects in resistive switching Ti/HfO_2/TiN Cells. J Appl Phys. 2014;115(20):204509
[15] Sowinska M, Bertaud T, Walczyk D, et al. Hard X-Ray photoelectron spectroscopy study of the electroforming in Ti/HfO_2-based resistive switching structures. Appl Phys Lett. 2012;100(23):233509
[16] Yoon J-W, Yoon JH, Lee J-H, et al. Impedance Spectroscopic analysis on Effects of partial oxidation of TiN bottom electrode and Microstructure of amorphous and

Crystalline HfO_2 thin films on their bipolar resistive switching. Nanoscale. 2014;6(12):6668–6678

[17] Choi M, Lyons JL, Janotti A, et al. Impact of Carbon and nitrogen impurities in high-κ Dielectrics on metal-oxide-semiconductor devices. Appl Phys Lett. 2013;102(14):142902

[18] Calka P, Sowinska M, Bertaud T, et al. Engineering of the chemical Reactivity of the Ti/HfO_2 interface for RRAM: Experiment and Theory. ACS Appl Mater & Interfaces. 2014;6(7):5056–5060

[19] Tanuma S, Powell CJ, Penn DR. Calculations of electron inelastic mean free Paths. V. Data for 14 Organic Compounds over the 50–2000eV Range. Surf Interface Anal. 1994;20(3):165–176.

[20] Niu G, Kim H-D, Roelofs R, et al. Material Insights of HfO_2-based integrated 1-Transistor-1-Resistor resistive random access memory devices Processed by Batch atomic layer deposition. Sci Rep. 2016;6:28155

[21] Morant C, Galán L, Sanz JM. An XPS study of the Initial Stages of oxidation of Hafnium. Surf Interface Anal. 1990;16(1–12):304–308

[22] Prieto P, Kirby RE. X-Ray photoelectron spectroscopy study of the Difference between Reactively Evaporated and Direct Sputter-deposited TiN films and their oxidation properties. J Vac Sci Technol A. 1995;13: 2819–2826

[23] Suni I, Sigurd D, Ho KT, et al. Thermal oxidation of Reactively Sputtered Titanium Nitride and Hafnium Nitride films. J Electrochem Soc. 1983;130(5):1210–1214

[24] Khan AI, Chatterjee K, Wang B, et al. Negative capacitance in a ferroelectric capacitor. Nat Mater. 2014;14:182

[25] Huang P, Liu XY, Chen B, et al. A Physics-based Compact model of metal-oxide-based RRAM DC and AC Operations. IEEE Trans Electron Dev. 2013;60(12):4090–4097